ORTHOPEDIC IMPLATJTS: MATERIAL AND FAILURE EVALUATION

by

W. Phucharoen

Submitted in Partial Fulfillment of the Requirements

for the Degree of

Master of Science in Engineering

in the

Materials Science Program

Richard W Jones 11 August 1983

Adviser Date

Sally M. Hotchkiss Aug 23, 1983

Dean of the Graduate School Date

Youngstown State University

August 1983

ORTHOPEDIC IMPLATJTS: MATERIAL AND FAILURE EVALUATION

by

W. Phucharoen

Submitted in Partial Fulfillment of the Requirements

for the Degree of

Master of Science in Engineering

in the

Materials Science Program

Richard W Jones 11 August 1983

Adviser **Date**

Sally M. Hotchkiss August 23, 1983

Dean of the Graduate School **Date**

Youngstown State University

August 1983

ABSTRACT

ORTHOPEDIC IMPLANT: MATERIAL AND FAILURE EVALUATION

W. PHUCHAROEN

Master of Science in Engineering

Youngstown State University, 1983

Two type 316 stainless steel orthopedic implants, Eggers plate and Jewett hip nail-plate, were examined in order to find the causes of failure. Unusual crack patterns were found on the cylindrical surface of the implants. Type 316 stainless steel tensile samples were tested with the presence of tensile stresses to determine the low-cycle fatigue characteristics and to determine whether or not low-cycle tensile stress would produce either of the crack patterns observed in the fractured implants.

it was found that the Eggers plate seems to fail because of bending fatigue and improper design. Low-cycle tensile stresses do not produce the crack pattern observed on the cylindrical surface of the Jewett nail-plate.

However, the most important result of this work is the significance of the presence of tensile mean stresses that occur during normal walking of a human which can significantly shorten the operation life of a type 316 stainless steel implant.

ACKNOWLEDGEMENTS

The author wishes to thank his adviser, Dr. R.W. Jones, Department of Chemical Engineering and Materials Science at Youngstown State University for guidance in this study.

TABLE OF CONTENTS

LIST OF FIGURES

LIST OF FIGURES (Cont'd)

FIGURE PAGE

LIST OF FIGURES (Cont'd)

FIGURE PAGE

LIST OF TABLES

CHAPTER 1

INTRODUCTION

An "implant" according to Gray (1962) is a device which is temporarily attached to a fractured bone as a structural support while the fracture mends [1]. The implant is removed once the fracture has mended. A "prothesis" is a device permanently attached to a bone.

The first recorded use of an implant was in 1562 when gold prothesis was used to close a defect in a cleft palate [2]. Ludwigson [3,4] has divided the history and development into the three periods: first use to 1825, 1825 to 1925, and 1925 to the present time. In the first period only pure metals such as gold, silver, and copper were used as implants. In the second period, pure metals were still used as implants. But surgical techniques were greatly improved which increased the success of the implant. In the third period, alloys with improved strengths were used as implants.

Before the latter part of the nineteenth century, use of metallic orthopedic implants probably resulted in frequent failure of the implant. Advances in mechanical design and metallurgical technology, updated sterillization practices and greater discrimination in materials' selection, have greatly decreased incidence of failure in these devices.

Failure (particularly mechanical fracture) is not, however, uncommon, as evidenced by the large volume of literature concerning analysis of failed orthopedic implants [5-9] Consequently, further researches are encouraged so that use of orthopedic implants can be improved.

The impetus for this work resulted from the examination of two orthopedic implants that failed in service. The failed devices were a Jewett hip nail-plate and an Egger onlay plate (Figure 1). Figure 2 is a sketch of how these two devices are attached to a leg bone. The two implants were examined with a scanning electron microscope (SEM) in order to determine the causes of the failures.

In both cases unusual crack patterns were observed. The Eggers plate exhibited numerous cracks and slip lines in the fracture surface. In the case of the Jewett hip nail-plate no cracks could be found in the fracture surface. However, many cracks existed in the cylindrical surface immediately adjacent to the fracture surface. Neither of these crack patterns has been previously reported in the literature concerning failed implants. The morphology of the two crack patterns suggested that either fatigue, stress corrosion, or a combination of these mechanisms caused the fractures in the two implants. The objectives of this research were to determine low-cycle fatigue characteristics of type 316 stainless steel, and to determine whether or not low-cycle tensile stresses would produce either of the

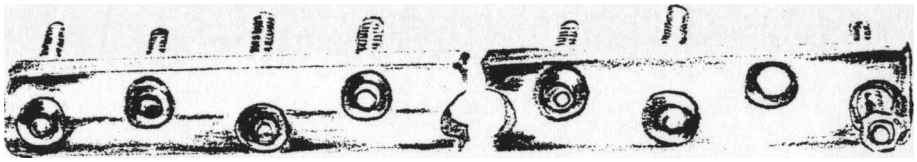

(a) Eggers Onlay Plate.

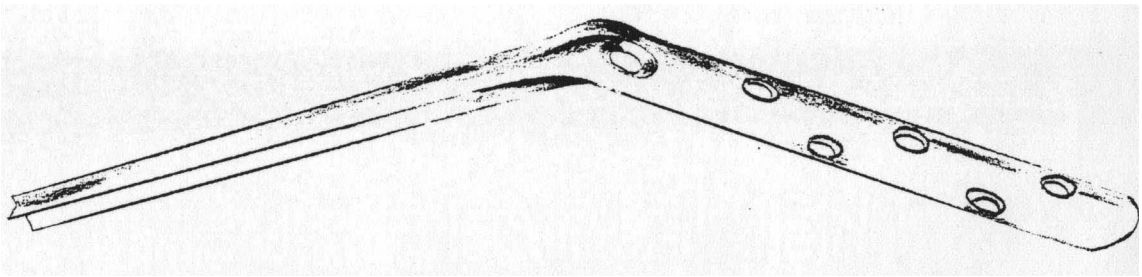

(b) Jewett Hip Nail-Plate.

Figure 1. Sketch of Eggers Onlay Plate and Jewett Hip Nail-Plate.

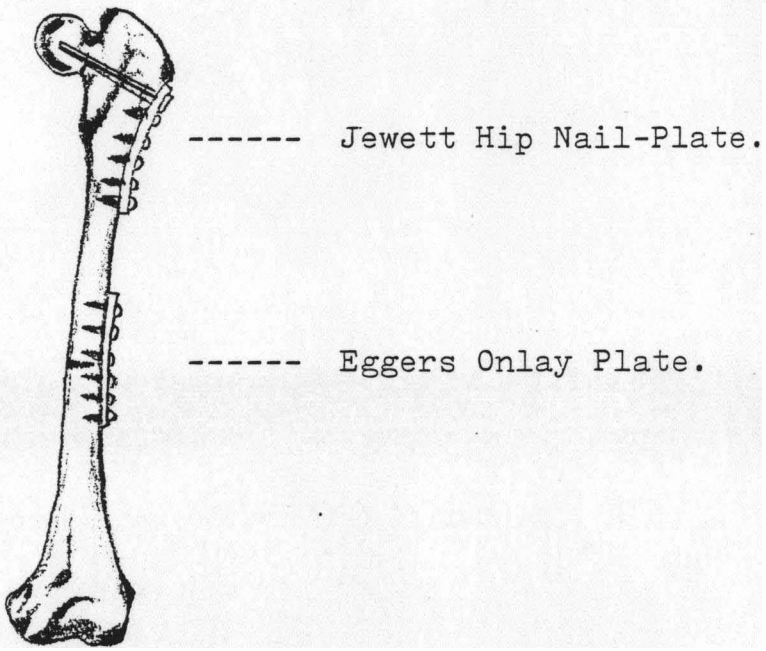

Figure 2. Sketch of How a Jewett Hip Nail-Plate and Eggers Onlay Plate are Attached to A Leg Bone.

crack patterns observed in the two fractured orthopedic implants.

CHAPTER II

LITERATURE REVIEW

A large number of articles have been published concerning the failure of orthopedic implants. Some of these are Ref. 5-8; and volume 10 of the Metals Handbook [9]. Dumbleton and Miller, devotes one chapter to the failure analyses of such devices. Generally, the failure of an implant cannot be attributed to only a single cause [10]. One major cause of an implant failure is related directly to the human body, which is considered to be one of the most hostile environments for metals. In the human body, chemical and electro-chemical reactions which may occur are not well identified or understood. Moreover, the problem of loading geometries involving cyclic loading can be encountered when dealing with particular areas of the musculo-skeleton system such as the hip or knee. The combination of the hostile or aggressive environment and stringent loading conditions have brought about two familiar problems: corrosion or fatigue and their interaction. Both of these phenomena have been identified as major contributors to deterioration of implants in service [16].

Implant failures can be related to five factors. They are (a) corrosion, (b) patient misuse, (c) materials selection, (d) improper installation of the implant and (e) design and

manufacture.

The first two factors listed concern directly with the environment. The other three factors are related to the implant and its installation into the body.

(a) Corrosion

The corrosion mechanisms which generally lead to degradation or failure of currently used implant devices, fretting enhanced crevice corrosion and stress-corrosion, are associated primarily with stainless steel usage. Stress-corrosion cracking has been recognized as a cause of implant failure. However, neither its identification nor its importance in most cases has been yet determined because the cyclic loading produced by the body movement almost always results in a fretted or striated fatigue or corrosion fatigue. Pitting and intergranular attack, considered as results of improper chemistry control or mechanical processing, are not yet observed in implants.

(b) Patient Misuse

This factor of implant failures is directly related to the role of the patient. Devices may fracture by overloading because of patient misuse. For example, if the patient falls, very heavy loads are placed on a fixation device. Ignoring instructions about weight limits that a device can bear is also hazardous to implants. The patient usually has little or no control over the forces that muscles exert on an implant. High loads may result even when a patient is confined to bed.(12)

(c) Material Selection

The right kind of materials for implants must be carefully selected because only a few alloys have the necessary combination of properties; otherwise, the implants may be dangerous to the patient's body (13)

For surgical implants, a bone plate and bone screw must be of similar metals so that galvanic corrosion can be avoided. Usually, the corrosion occurs between the plate and the underside of the screw heads. The importance of material selection is exemplified by Dumbleton and Miller. They studied an example of a nail-and-plate device made of cast and wrought cobalt-chromium alloys which fractured as a result of dissimilar-metal contact, stress concentration and crevice corrosion (14)

Type 316 stainless steel was finally selected for surgical implants since the second world war (15). It became the desired metal for surgical implants basically because of its high pitting corrosion resistance. The composition and microstructural variations affect more or less the resistance of type 316 stainless steel to pitting corrosion. The addition of 2-4 percent of molybdenum in composition has proved to greatly reduce sensitiveness to this kind of attack in an environment containing chloride (16) Warren (17) revealed that pitting corrosion resistance can be decreased with cold work by promoting, along strain lines, the formation of second phase constituents.

(d) Improper Installation of Implant

Faiiure of an implant may result from nonoptimal installation. Occasionally, the most desirable device is not possibly available for immediate surgical use. For instance, the surgeon may be forced to improvise, encountering the crucial situation when the operating room runs out of the stock for a particular item.

Some failures can be attributed to errors in technigue For example, some errors in insertation include use of inappropriate size of implant parts (either too large or too small a screw, a nail or a plate) or use of eccentric or misaligned screws.

Improper installation of implant can be caused bv over applying torque to bone screws. The other aspect of improper installation is when the head of the screw is not sheared-off immediately. The implant failure may occur later because the screw becomes weak (18)

(e) Design and Manufacture

At the stage of implant fabrication, high quality control must be carefully exerted in the type of finish om-the fixation device. The surface must not be blemished cf machining marks that could influence stress raisers which eventually activate a fissure and subsequent fractures (19)

Premature features can be attributed to the design-of an implant. For instance, sharp corners of an implant can result in stress raisers and lead finally to

fracture. In addition, the failure can come from screw holes which were punched too close to the edge of a bone plate. The plate is, thus, not able to withstand bending stresses[20].

CHAFTER III

EXPERIMENTAL PROCEDURE

Two implants, a Jewett hip nail-plate and a Eggers onlay plate, were sectioned about half an inch from the fracture surface using silicon-carbide wheel. A scanning electron microscope (SEM) Model S-450 (Hitachi) was used to examine fracture surfaces and cylindrical surfaces of each implant specimen. For the Jewett hip nail-plate, the fracture surface was also examined by metallographic examinations.

Standard 0.505 inch diameter tensile samples of type 316 stainless steel used for this study were purchased from Laboratory Devices Co., Auburn, California.

One tensile sample was used to measure the mechanical properties (see Table 1) with Model M120 HVL, Satec System Inc., Grove City, PA., tension testing machine.

The remaining samples had a 0.005 inch cylindrical grove machined in the center of the gauge length in order to generate a stress concentration (see Figure 3). Without the stress concentration, fatigue failure would take a long period of time. Each sample was cycled in uniaxial tension on an MTS electrohydraulic tesing machine with different amplitude load and load range. Sinusoidal wave forms were employed for the loading, with the expectation

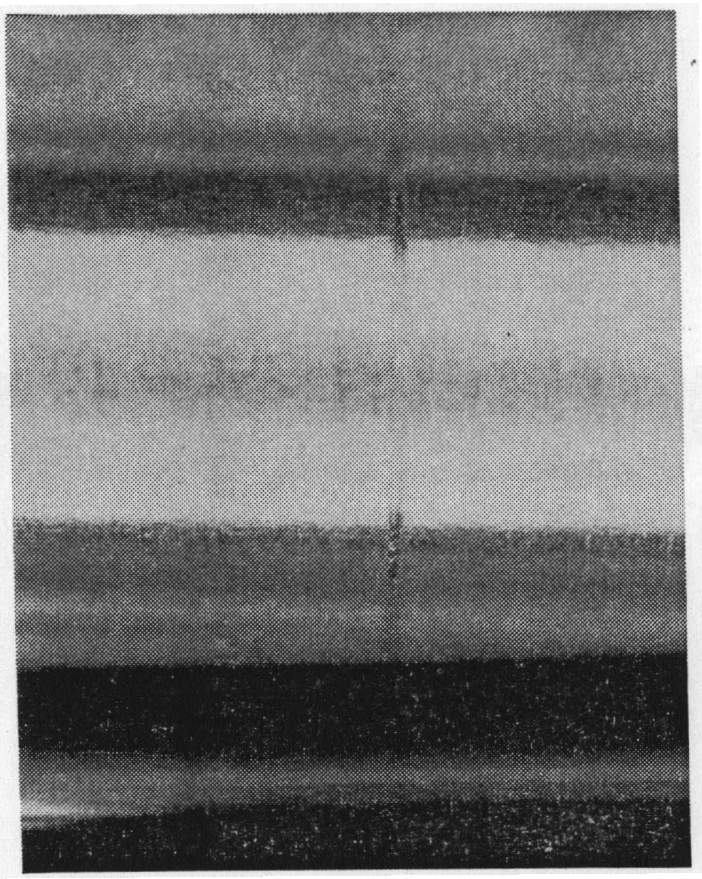

Figure 3. Show Machine Scratch on a Type 316 Stainless Steel Tensile Sample. 36X.

TABLE 1

MECHANICAL PROPERTIES OF TYPE 316 STAINLESS STEEL

Offset yield strength	69,750 psi
Ultimate tensile strength	95,400 psi
Elongation	46.9%

that wave forms would have little effect on tests carried out in air at room temperature [21]. The test data are listed in Table 2 and a plot of stress amplitude (S_a, psi) versus numbers of cycles to failure (S-N diagram) is shown in Figure 4. Also, the accepted fatigue curve for type 316 stainless steel [22] is plotted on the same graph (see Figure 4).

The fractured samples were examined on the SEM. Their fracture surfaces were photographed (see Figures 5-12) in order to determine the ratio of the ductile fracture area to the total fracture area (see Table 3).

TABLE 2

TEST DATA OBTAINED FROM MTS TESTING MACHINE

Sample No.	Load (lbs.)	Frequency (cps)	No. of cycles to failure
1	14,000 ± 2,000	1	29,376
2	12,000 ± 3,000	1	22,456
3	9,000 ± 4,000	1	6,965
4	8,000 ± 5,000	1	764
5	14,000 ± 4,000	1	6
6	16,000 ± 2,000	1	66
7	12,000 ± 4,000	1	14
8	9,000 ± 2,000	8	No failure
9	9,000 ± 6,000	1	14

TABLE 3

CALCULATED DATA OBTAINED FROM TABLE 2

Sample No.	Stress (psi)	Cycles to Failure	Amplitude Stress (psi)	Mean Stress (psi)	Ratio of Ductile Area to Total Fracture Area
1	72,765 + 10,395	29,376	72,765	10,395	0.20
2	62,370 + 15,593	22,456	62,370	15,593	0.28
3	46,778 + 20,790	6,965	46,778	20,790	0.28
4	41,580 + 25,988	764	41,580	25,988	0.17
5	72,765 + 20,790	6	72,765	20,790	1.00
6	83,160 + 10,395	66	83,160	10,395	1.00
7	62,370 + 20,790	14	62,370	20,790	1.00
8	46,776 + 10,395	No failure	46,778	10,395	----
9	46,778 + 31,185	14	46,776	31,185	1.00

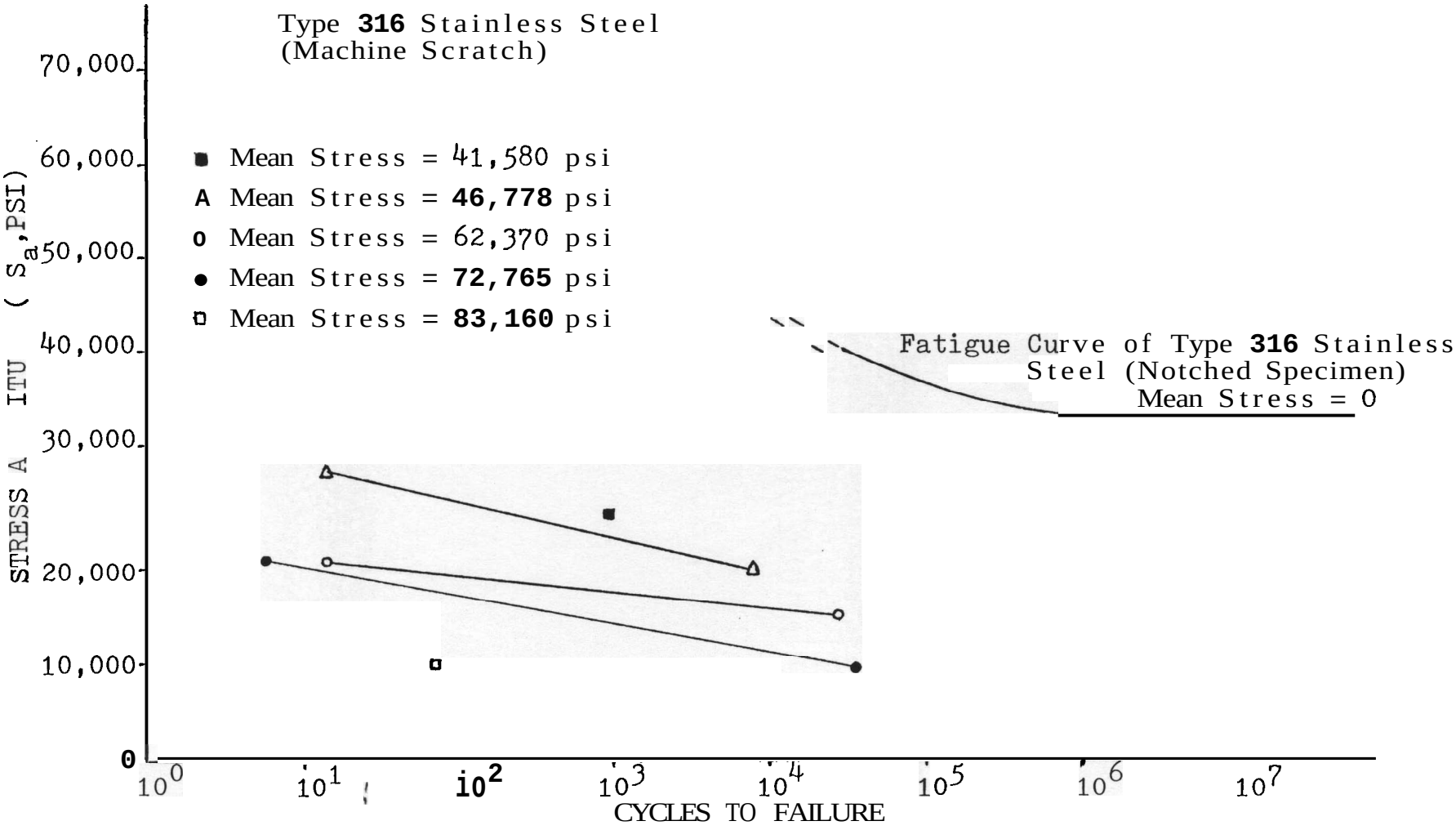

Figure 4. Graph Plotted Between Stress Amplitude (S_a,psi) VS. Cycles to Failure.

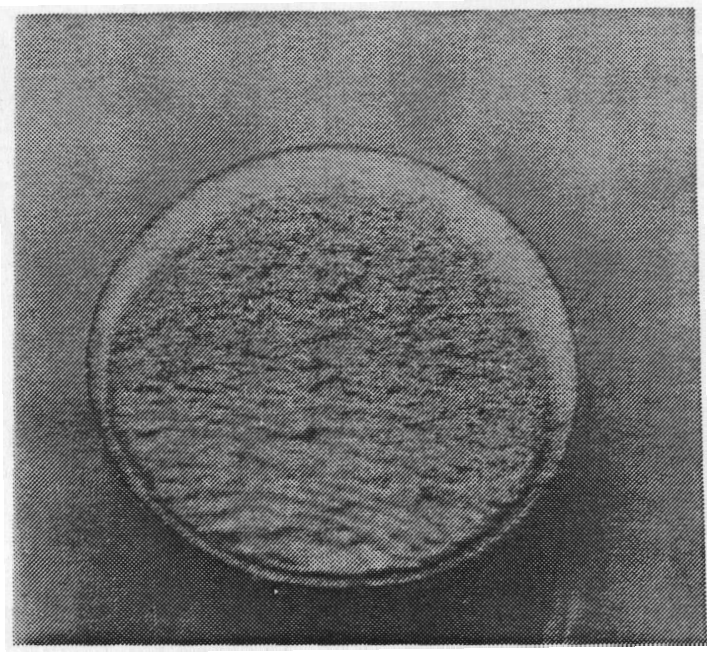

Figure 5. Fracture Surface of Sample No. 1. 36X.

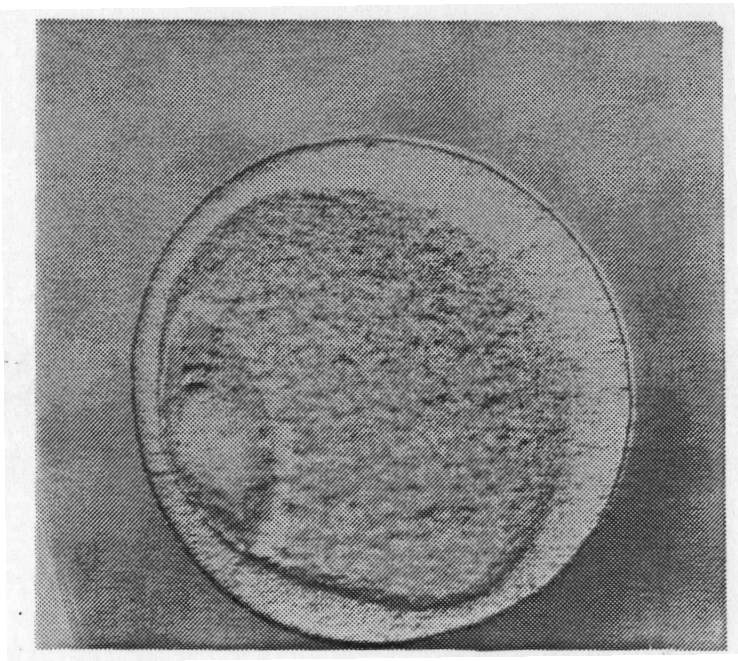

Figure 6. Fracture Surface of Sample No. 2. 36X.

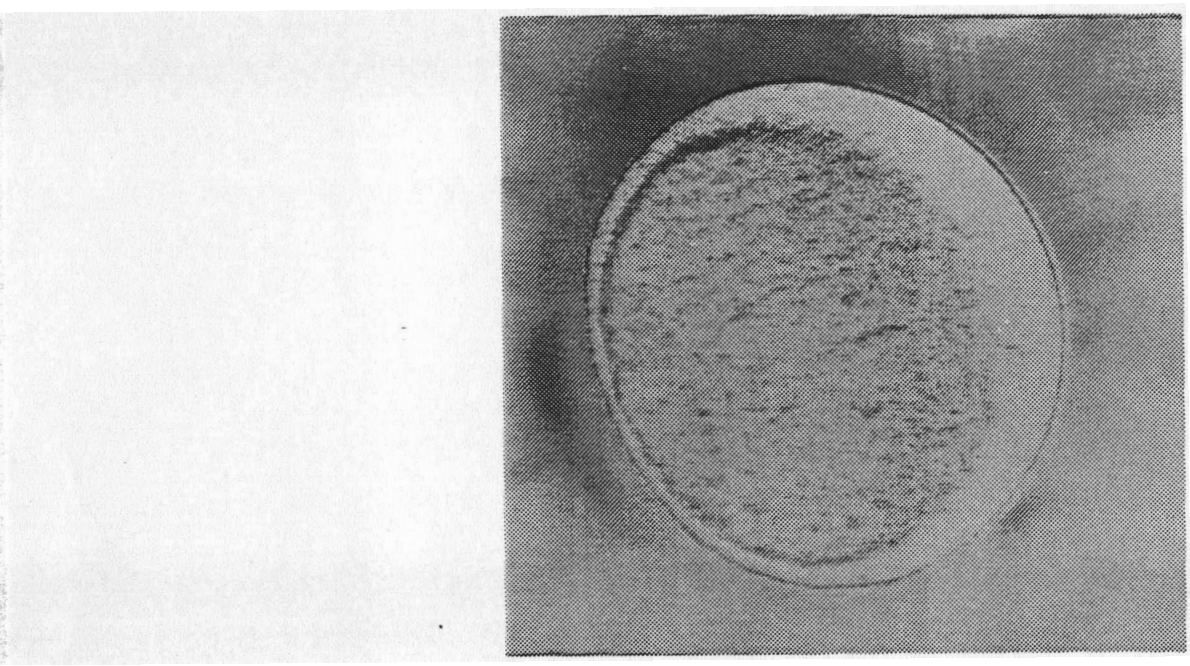

Figure 7. Fracture Surface of Sample No. 3. 36X.

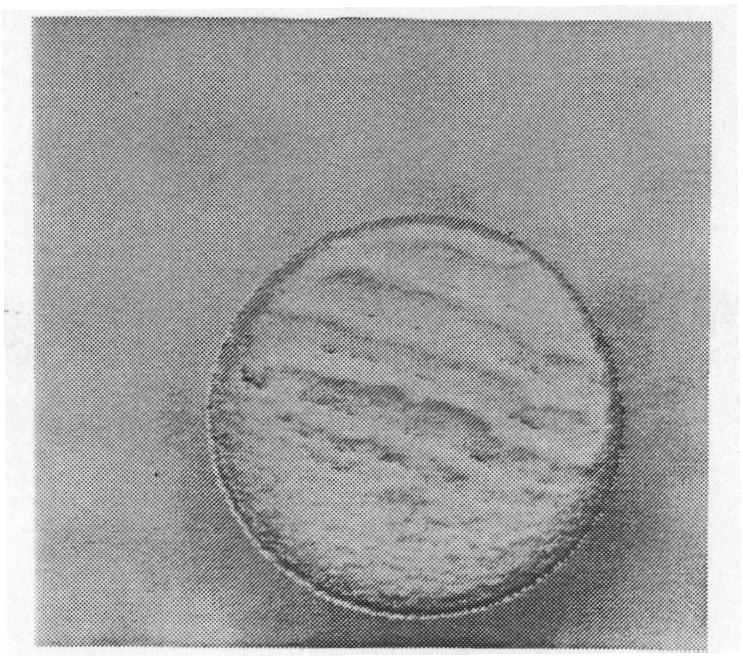

Figure 8. Fracture Surface of Sample No. 4. 36X.

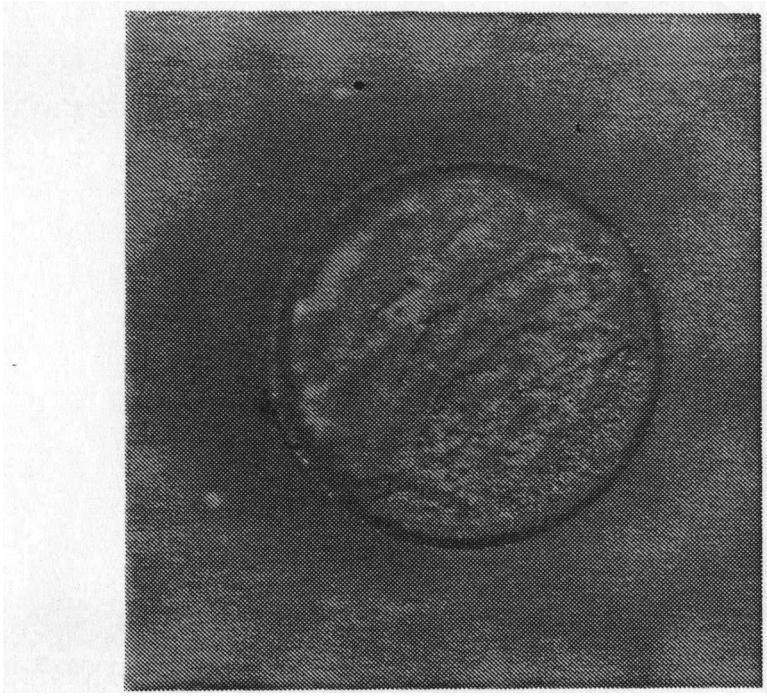

Figure 9. Fracture Surface of Sample No. 5. 36X.

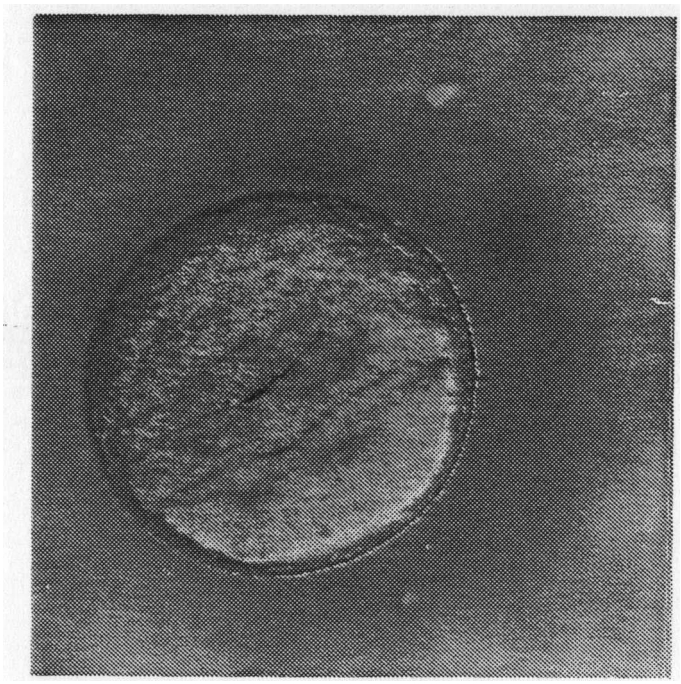

Figure 10. Fracture Surface of Sample No. 6. 36X.

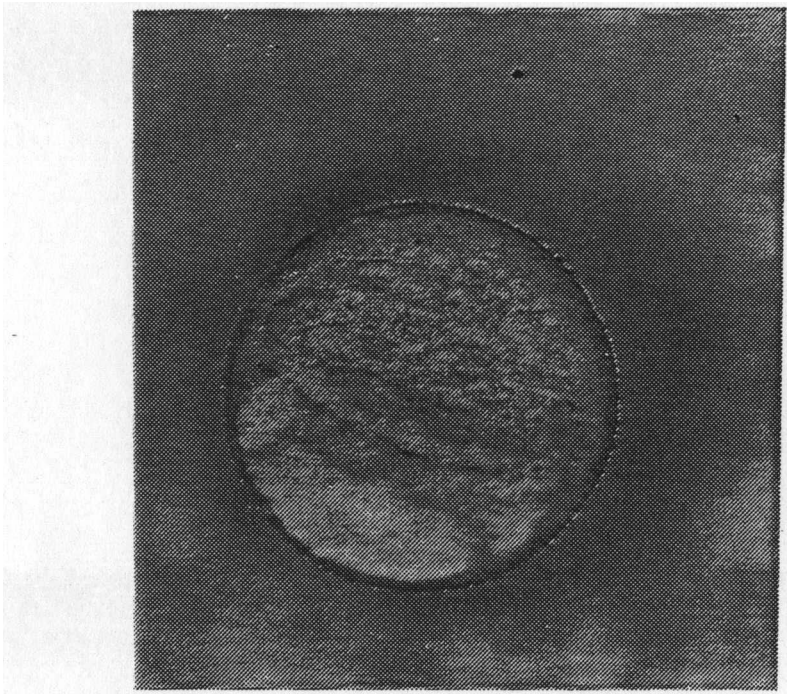

Figure 11. Fracture Surface of Sample No. 7. 36X.

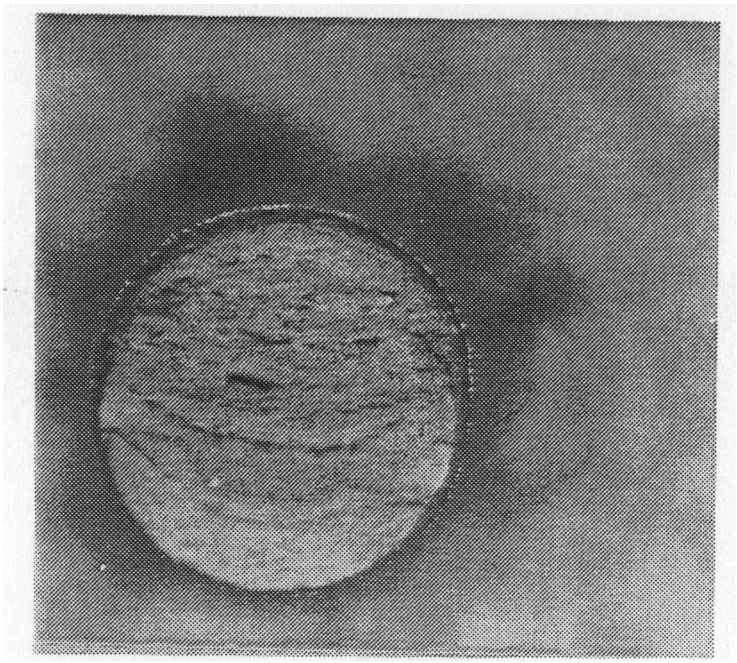

Figure 12. Fracture Surface of Sample No. 9. 36X.

CHAPTER IV

RESULTS AND DISCUSSION

The results are discussed in two sections, microstructural analysis and fatigue analysis.

(a) Microstructural Analysis

Macroscopic examination of the Eggers plate revealed no evidence of corrosion in the vicinity of the fracture. Microscopic examination revealed numerous cracks in the fracture surface (see Figures 13–15). Figures 16–18 show the micrographs of this device through fractured area. There was no evidence of stress-corrosion. By comparing Figure 15 and Figure 16, both pictures having been taken at the same magnification and in the same area, it was found that the crack pattern of the fracture surface (Figure 16) was not intergranular corrosion pattern since the grain size in Figure 15 was larger. Gray and Zirkle (23) showed in their examination of type 316 stainless steel Jewett nail that grain size of intergranular corrosion pattern and microstructure near the fracture are similar.

The holes in this device were punched too close to the edge (see Figure 2). A reduced cross section can make a stress riser in the area where high stresses would occur during walking, and cracks would initiate and propagate. Cahoon and Paxton (24) show that the entire section of the

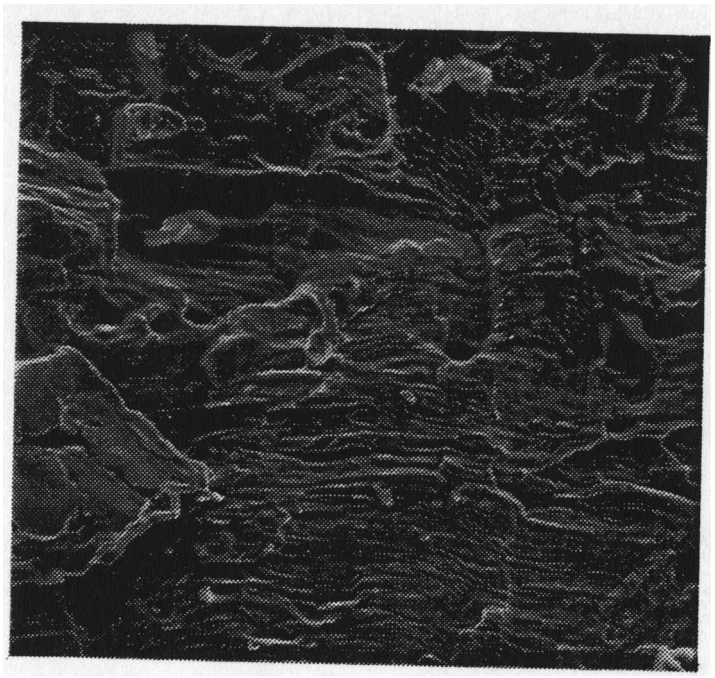

Figure 13. SEM Fractograph at 600X of Fracture Surface of Eggers Plate.

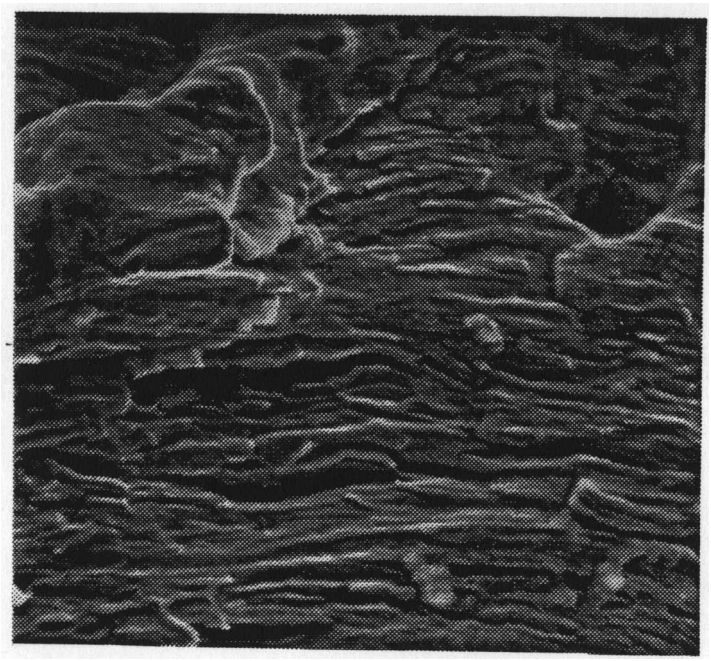

Figure 14. SEM Fractograph at 1200X of Fracture Surface of Eggers Plate.

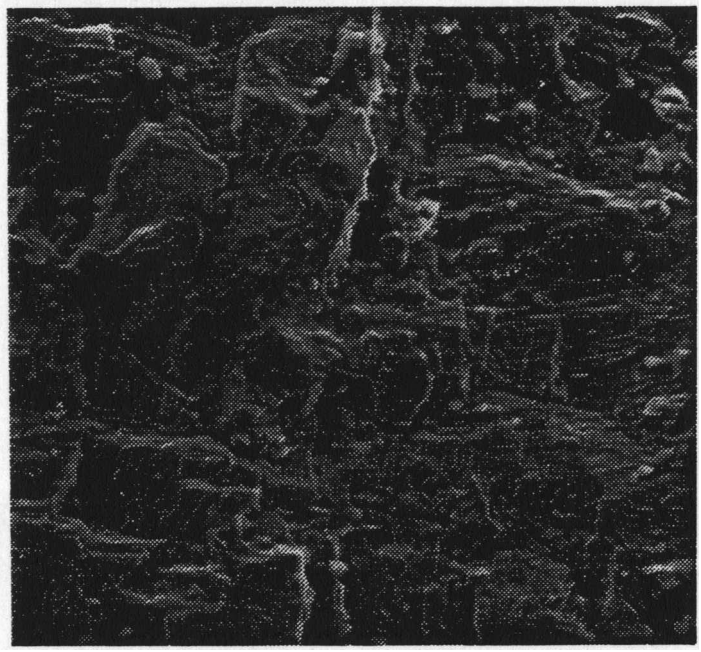

Figure 15. SEM Fractograph at 600X of Fracture Surface of **Eggers** Plate.

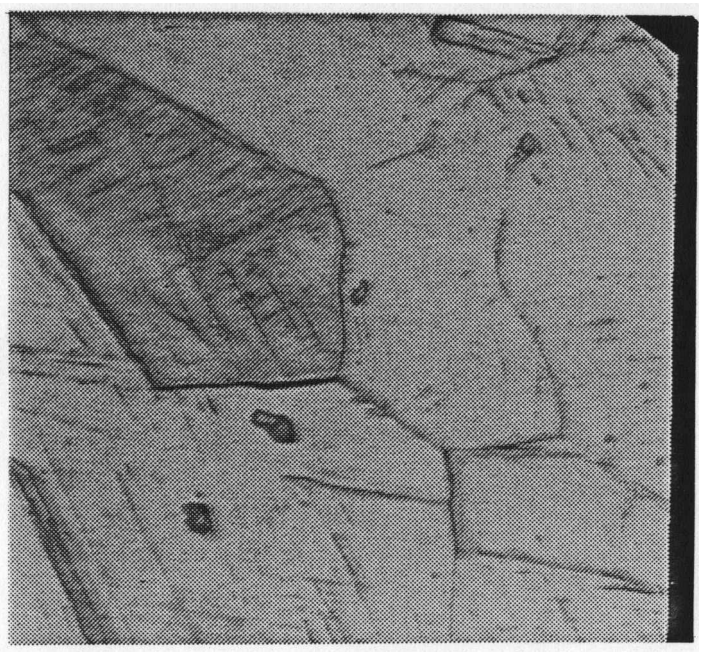

Figure 16. Micrograph of Eggers Plate Through Failure Area. 600X.

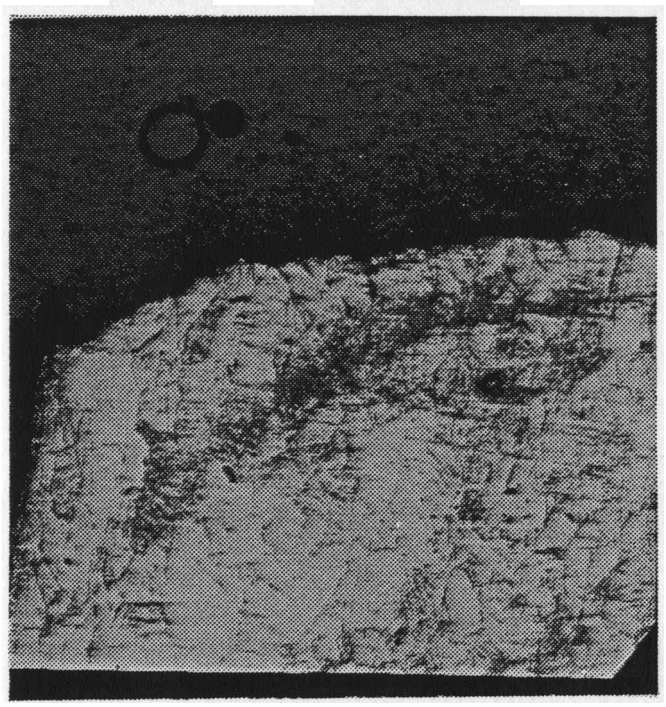

Figure 17. Micrograph of Eggers Plate Through Failure Area. 75X.

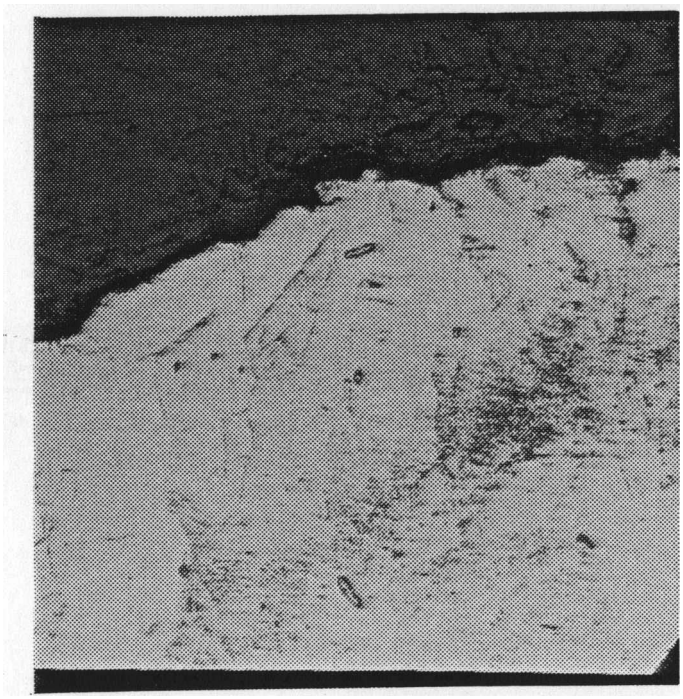

Figure 18. Micrograph of Eggers Plate Through Failure Area. 150X.

plate (type 316 stainless steel nail plate) between the hole and the edge is severely work hardened and much martensite forms. Their picture of plastic deformation and martensite in the plate is similar to Figures 16-18. The areas between the holes and edge of the plate, which have been severely deformed, may fracture with only a small amount of bending because both work-hardened material and martensite are harder and more brittle than the less work-hardened and un-transformed austenite which constitutes most of the implant.

Also, slip bands and associated microcracks pattern shown in Figure 14 are similar to what Ligasor [25] found on a surface of a type 316 stainless steel Jewett nail. Results from this examination indicate extensive deformation and accelerated fatigue were chosed by the large grain size of the device.

Therefore, the design of the implant seems to be the major cause of failure in the Eggers plate.

In the case of Jewett hip nail-plate the fracture surface was so badly disturbed that the cause of failure could not be determined from either a SEM or metallographic examination. A most unusual crack pattern was, however, found on the cylindrical surface immediately adjacent to the fracture surface (see Figures 19-22).

Figures 23-28 show the crack patterns found on the cylindrical surfaces immediately adjacent to the fracture surfaces of the samples tested under low-cycle tension.

Figure 19. Crack Pattern Found on Cylindrical Surface of Jewett Hip Nail-Plate (SEM), at 400X.

Figure 20. Crack Pattern Found on Cylindrical Surface of Jewett Hip Nail-Plate (SEM), at 450X.

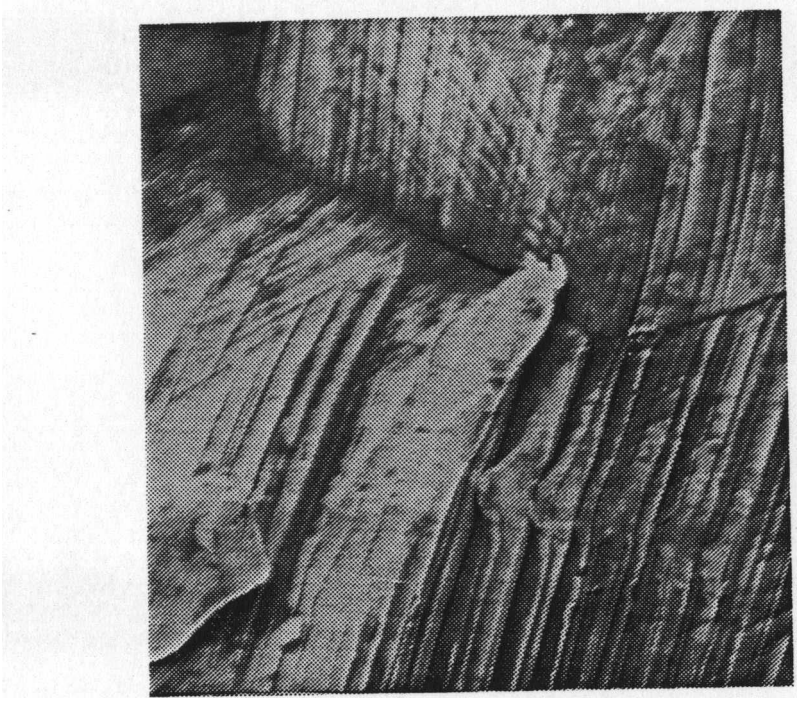

Figure 21. Crack Pattern Found on Cylindrical Surface of Jewett Hip Nail-Plate (SEM), at 1200X.

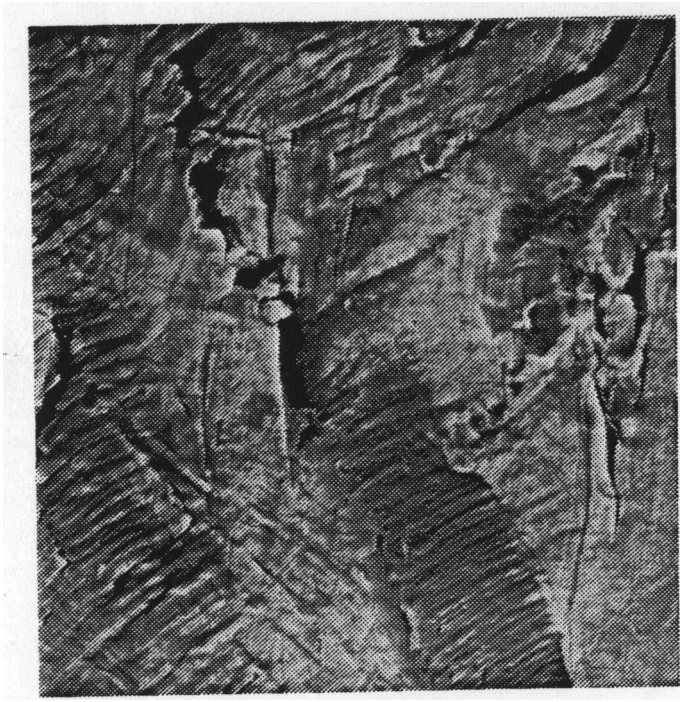

Figure 22. Crack Pattern Found on Cylindrical Surface of Jewett Hip Nail-Plate (SEM), at 1200X.

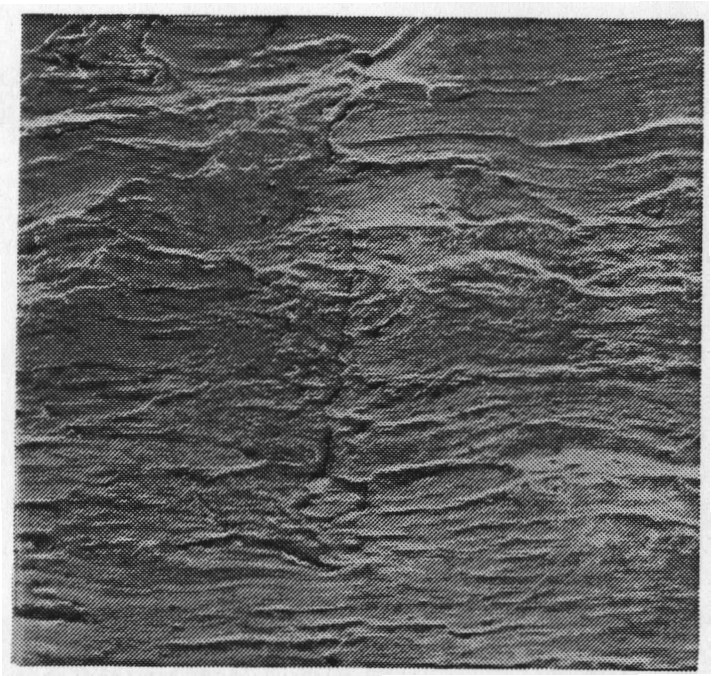

Figure 23. Crack Pattern Found on Cylindrical Surface of Sample No. 1. (SEM), at 500X.

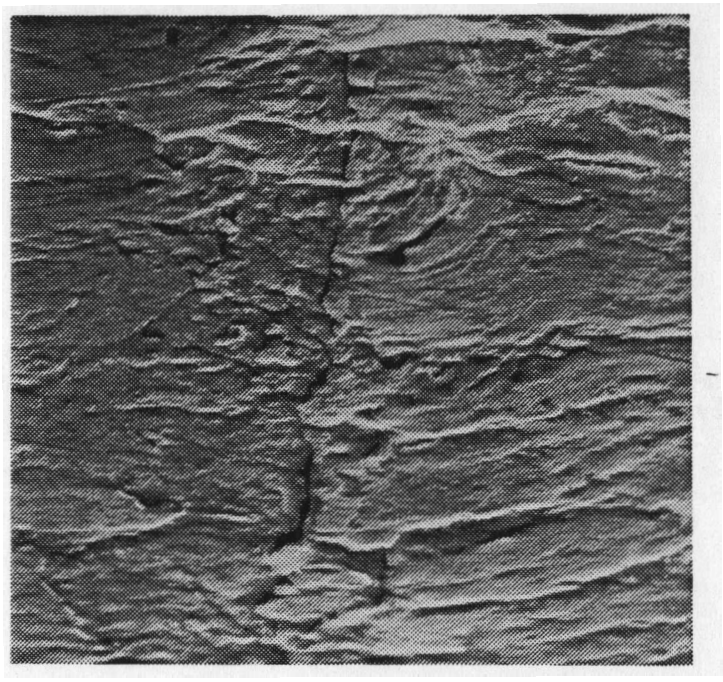

Figure 24. Crack Pattern Found on Cylindrical Surface of Sample No. 1. (SEM), at 800X.

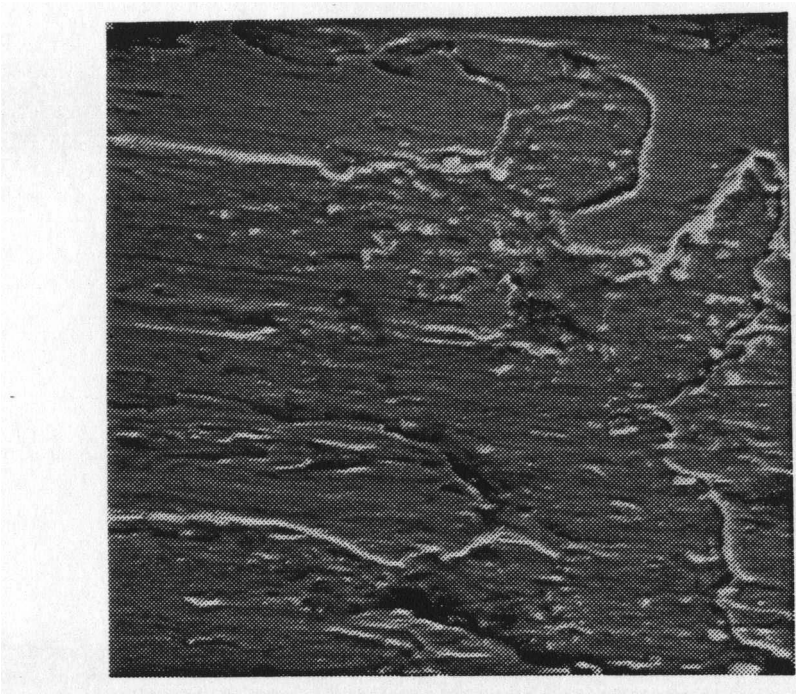

Figure 25. Crack Pattern Found on Cylindrical Surface of Sample No. 2.(SEN), at 820X.

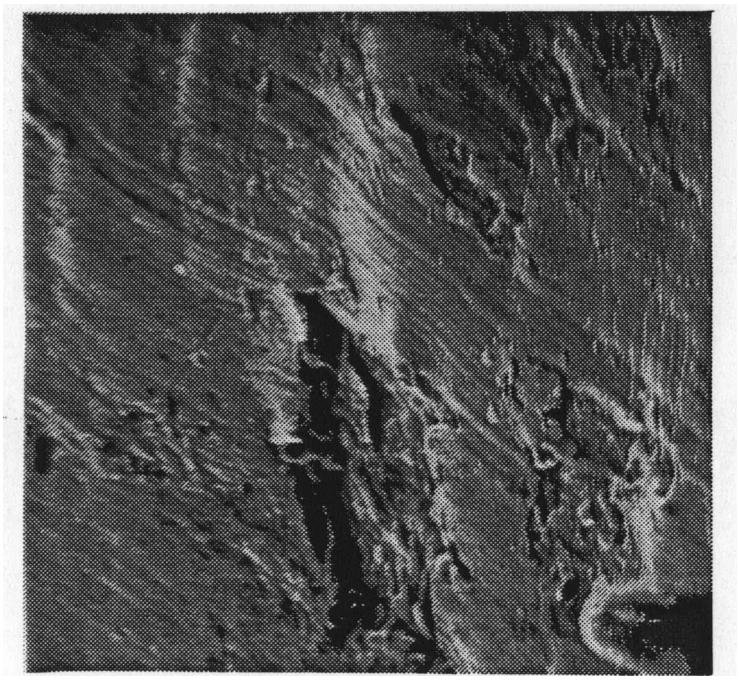

Figure 26. Crack Pattern Found on Cylindrical Surface of Sample No. 2.(SEM), at 870X.

Figure 27. Crack Pattern Found on Cylindrical Surface of Sample No. 3. (SEM) ~ 380X.

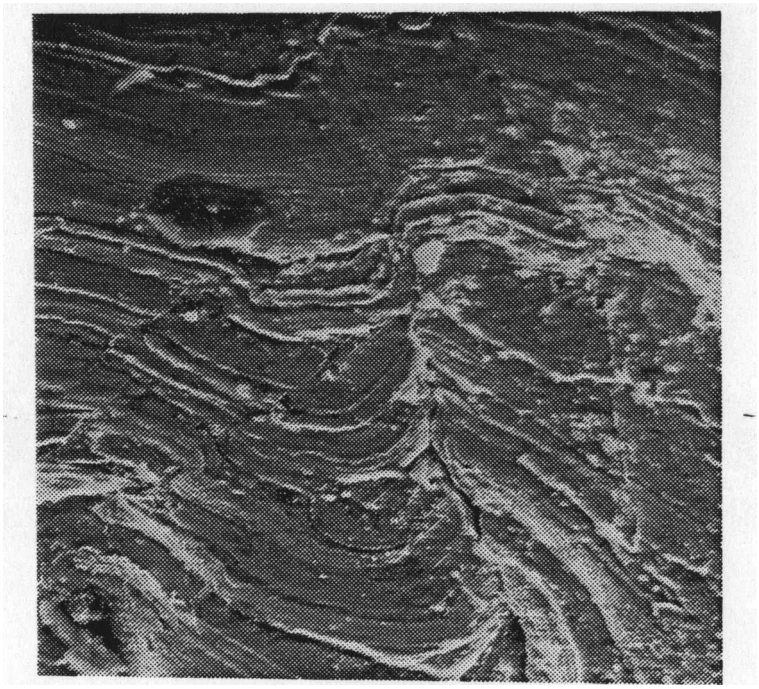

Figure 28. Crack Pattern Found on Cylindrical Surface of Sample No. 3. (SEN'), at 840X.

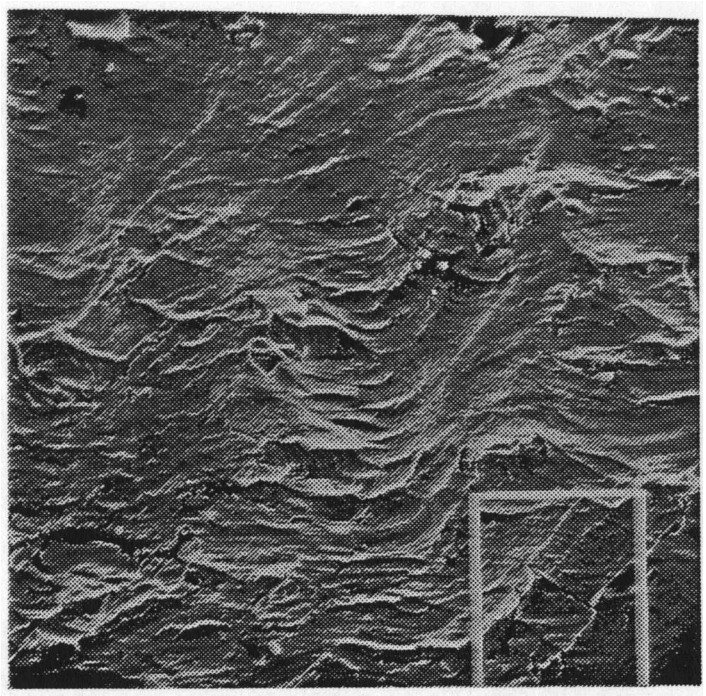

Figure 29. Crack Pattern Found on Cylindrical Surface of Sample No. 4. (SEM), at 400X.

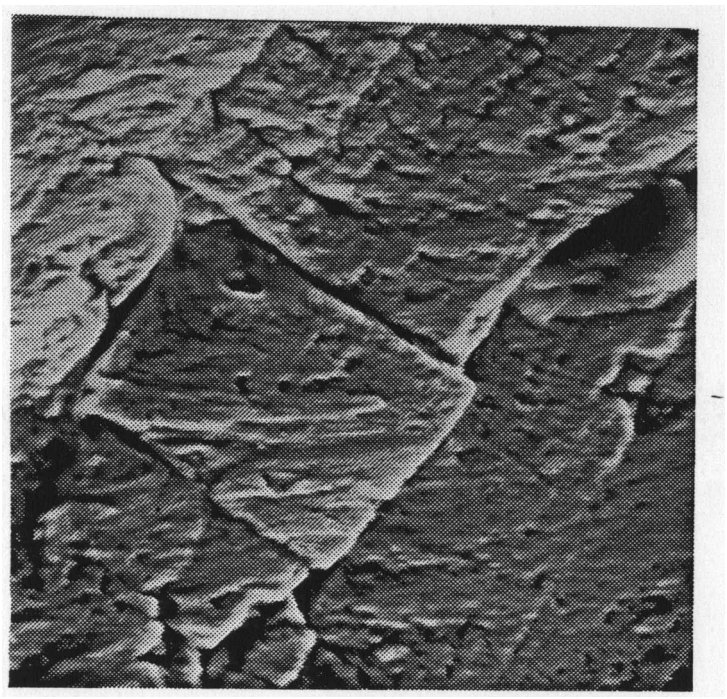

Figure 30. Crack Pattern Found on Cylindrical Surface of Sample No. 4. (SEM), at 2000X.

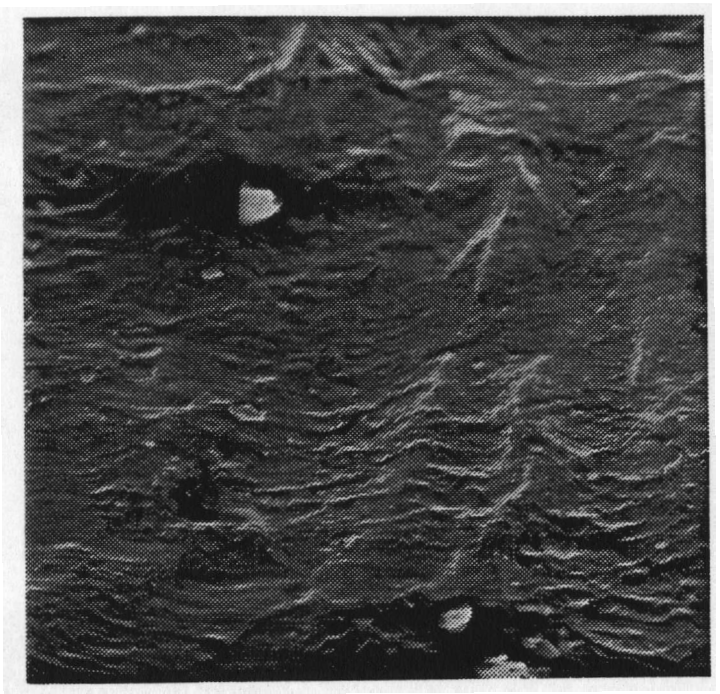

Figure 31. Crack Pattern Found on Cylindrical Surface of Sample No. 5. (SEM), at 400X.

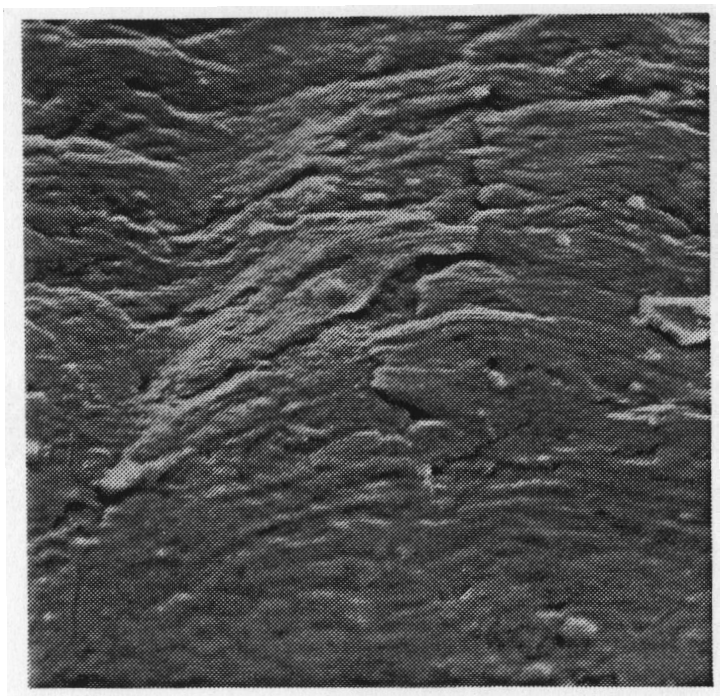

Figure 32. Crack Pattern Found on Cylindrical Surface of Sample No. 5. (SEM), at 1400X.

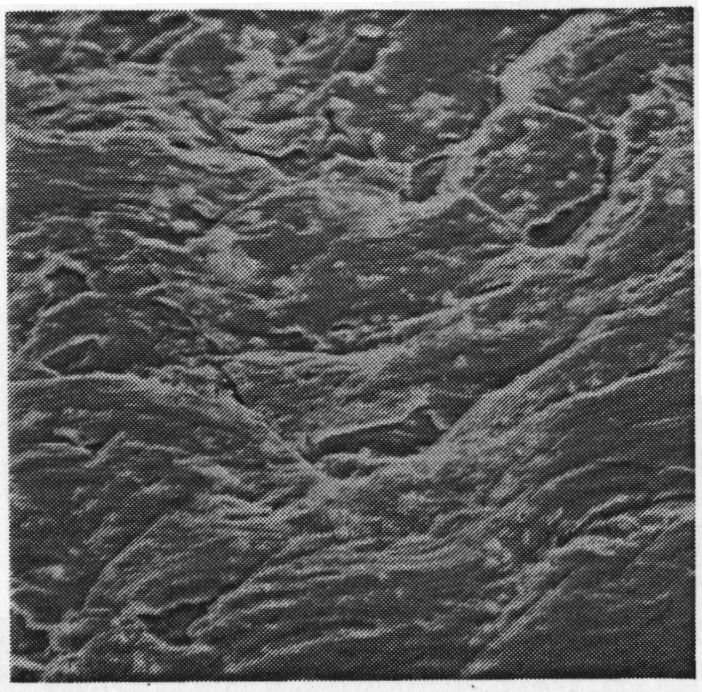

Figure 33. Crack Pattern Found on Cylindrical Surface of Sample No. 6. (SEM), at 100X.

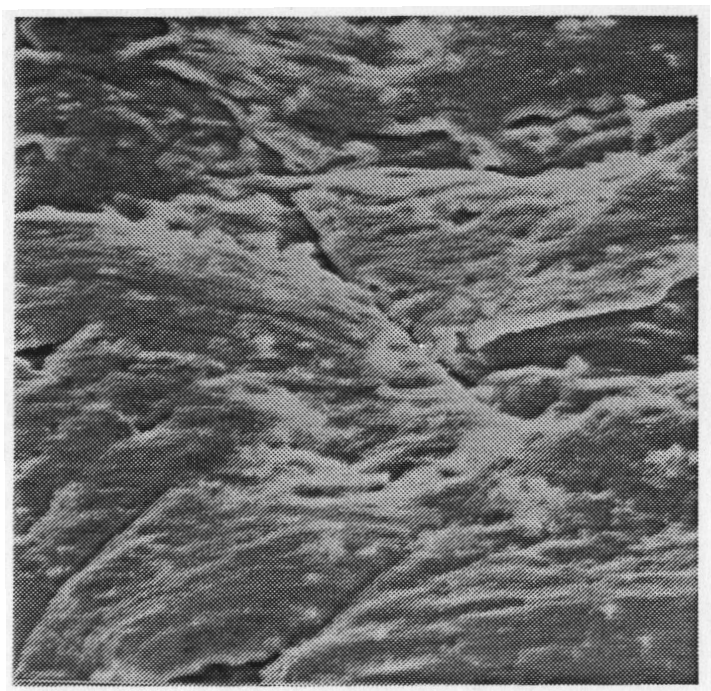

Figure 34. Crack Pattern Found on Cylindrical Surface of Sample No. 6. (SEM), at 1900X.

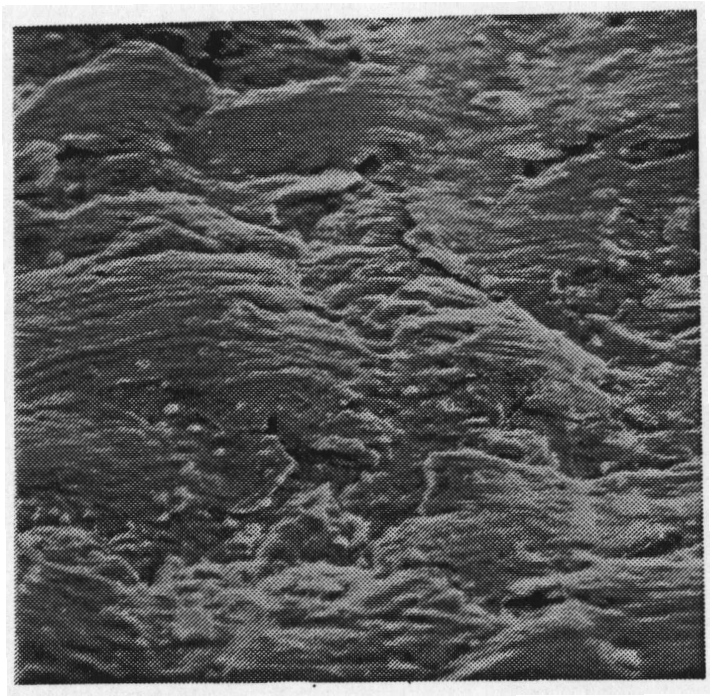

Figure 35. Crack Pattern Found on Cylindrical Surface of Sample No. 7. (SEM), at 800X.

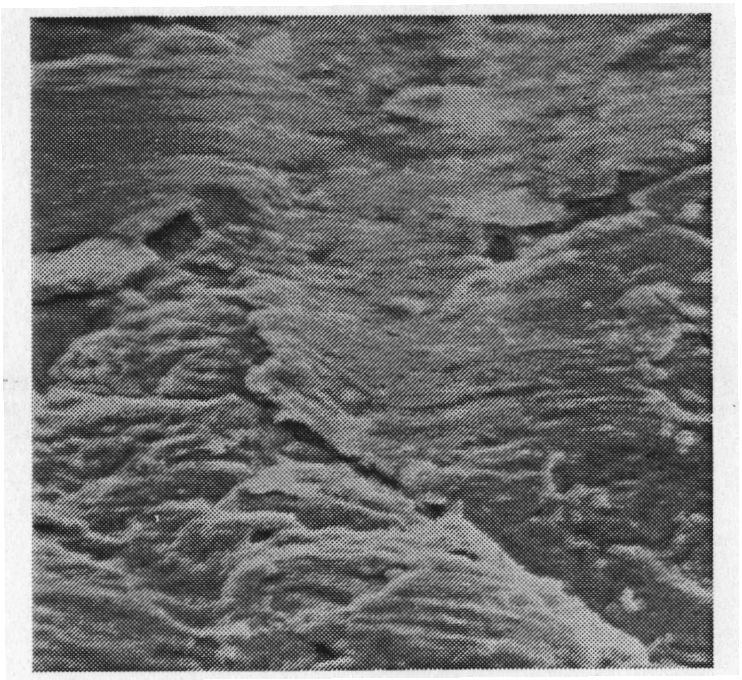

Figure 36. Crack Pattern Found on Cylindrical Surface of Sample No. 7. (SEM), at 1600X.

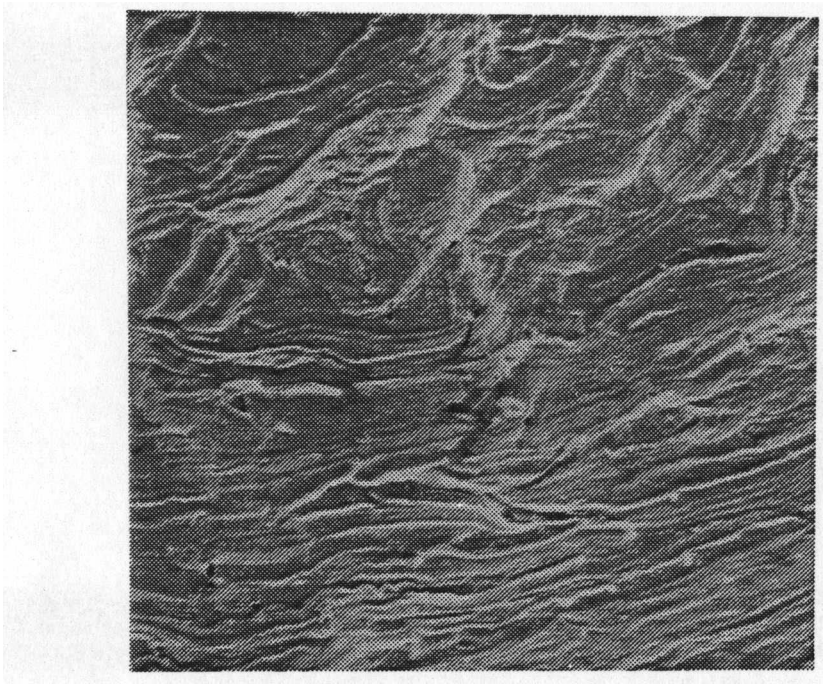

Figure 37. Crack Pattern Found on Cylindrical Surface of Sample No. 9. (SEM), at 500X.

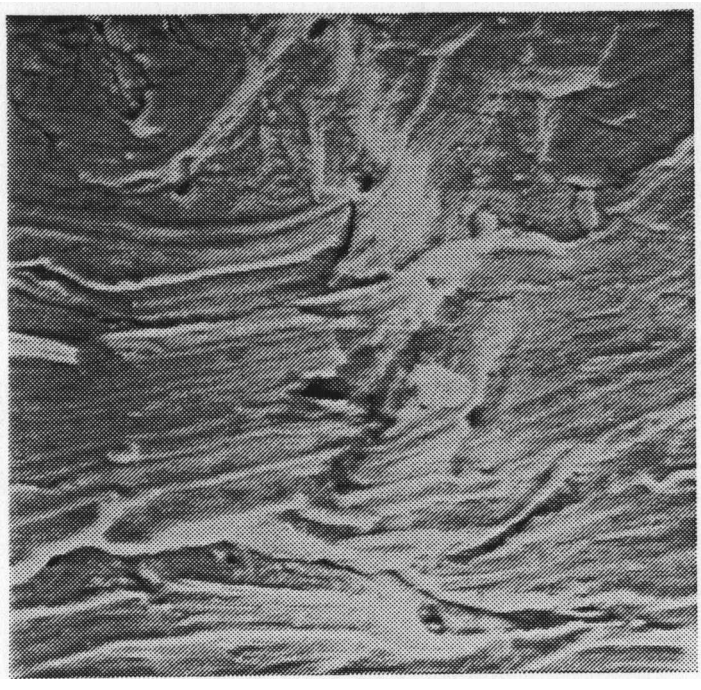

Figure 38. Crack Pattern Found on Cylindrical Surface of Sample No. 9. (SEM), at 1000X.

None of these crack patterns is similar to what we found on Jewett hip nail-plate. This means that a simple low-cycle tension stress was not the cause of failure of this device.

(b) Fatigue Analysis

Fatigue surfaces of samples no. 1-4 are typical fatigue patterns (see Figures 5-8). Figures 39 and 40 show fatigue striations of samples no. 1 and 4 respectively on the fracture surface. A ductile pattern, caused by a high stress in a low number of cycles to failure, was found on each fracture surface of samples no. 5-7 and 9 (see Figures 9-12). As listed in Table 3, the ratio of ductile area to total fracture area increases as the mean stress increases. Since the ductile area (final fracture area) depends on the stress in the last cycle, a larger ductile area is produced by a larger mean stress.

The accepted fatigue curve [26] of type 316 stainless stainless steel (notched specimen) was plotted in Figure 4 along with the results of this work in order to compare with the fatigue curves obtained in this experiment.

Since the largest part of the published fatigue data was obtained from fully reversed cycling (mean stress is zero) [27], a family of curves were plotted with each line corresponding to a different mean stress, as shown in Figure 4, on the S-N diagram. The curves show that increased mean tensile stresses severely decrease the fatigue life of type 316 stainless steel (samples no. 3,

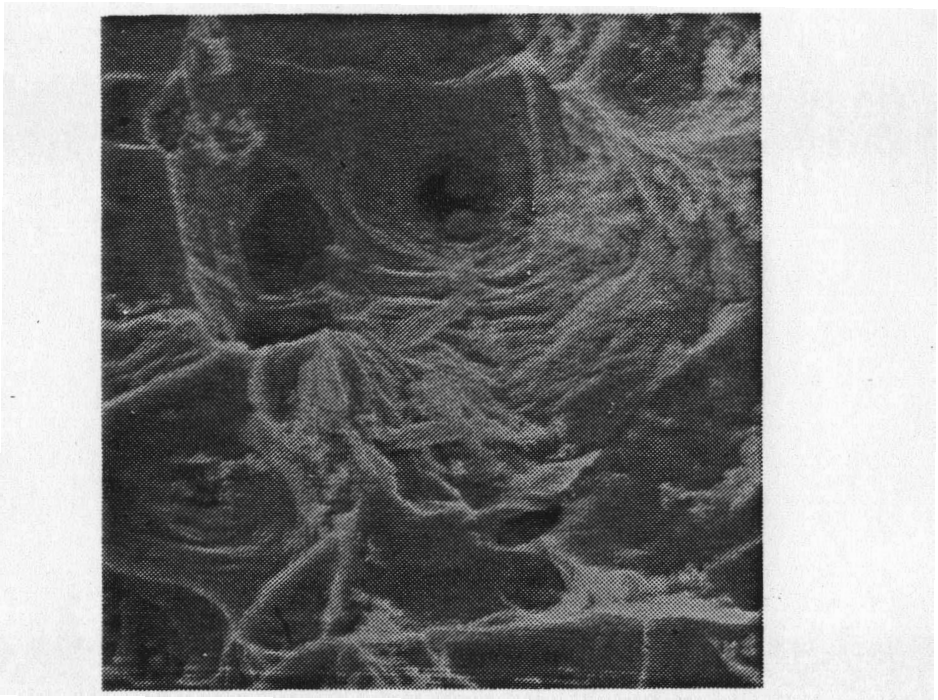

Figure 39. SEM Fractograph at 4500X of Fracture Surface of Sample No. 1 , Showing Fatigue Striations.

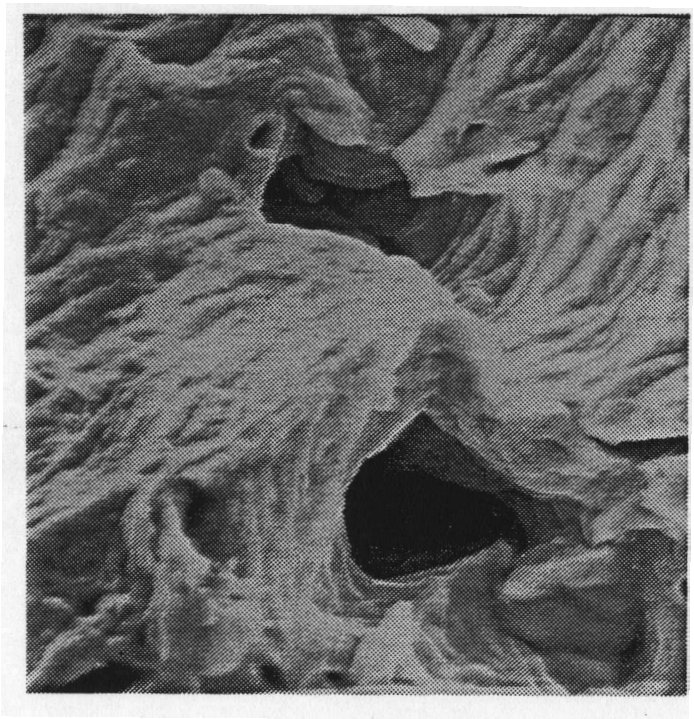

Figure 40. SEM Fractograph at 4400X of Fracture Surface of Sample No. 4 , Showing Fatigue Striations.

5 and 7). The fatigue curve of samples no. 3, 8 and 9 (mean stress of 47 ksi) shows that the endurance limit was reduced to about half of the actual endurance limit (no mean stress).

Sander [28] stated that these curves (in Figure 4) are not necessarily parallel to each other and it is not easy to predict the fatigue strength as influenced by mean stresses. Several empirical relations have been proposed but they are good only for the simple problems [29]

A square wave cycle was used to approximate the force time profile of a human leg during normal level walking [30]. It was found that the mean stress during each square wave cycle is tensile since compressive forces which are a small part of the total range do not appear to influence the propagation of fatigue cracks [31]

By combining the above fact with that type 316 stainless steel is very sensitive to presence of tensile mean stresses. It can be pointed out that any design and manufacture of type 316 stainless steel orthopedic devices must also consider these facts.

CHAPTER V

CONCLUSION

Type 316 stainless steel is very sensitive to the presence of mean stresses. Tensile mean stresses can severely reduce its fatigue life at a given amplitude of loading in air at room conditions.

Low-cycle tensile stresses do not produce the crack pattern observed in the two implants. For the Eggers plate, the failure seems to be a combination of improper design and bending fatigue. In the case of Jewett nail, failure may have been due to overload which resulted from bending stresses. It is fairly certain that low-cycle tensile loads did not cause either implant to fail.

The most important result of this work is the significance of the presence of tensile mean stresses that occur during normal walking of a human. Such stresses can markedly shorten the operation life of a type 316-stainless steel implant.

APPENDIX

Sample Calculation for Table 3

Sample No. 1

Mean Load	=	14,000	lbs.
Amplitude Load	=	2,000	lbs.
Diameter (initial)	=	0.495	inch
Mean Stress	=	$\frac{\text{Mean Load}}{\text{Area}}$	
	=	$\frac{14{,}000 \text{ lbs}}{0.192 \text{ sq. in.}}$	
	=	72,765	psi
Amplitude Stress	=	$\frac{2{,}000 \text{ lbs}}{0.192 \text{ sq. in.}}$	
	=	10,395	psi

REFERENCES

1. R.J. Gray, Failure analyses of Surgical Implants from the Human Body can Improve Product and Performance Reliability, Research Sponsored by Union Carbide Corporation under Contact with Energy Research and Development Administration, 1978, p. 1.
2. J.K. Wickstrom, Surgical Implants–Their Mechanical and Environmental Problems, Journal of Materials, Vol. 1, No. 2, June 1966, p. 367.
3. D.C. Ludwigson, Requirement for Metallic Surgical Implants and Prosthetic Devices, Metals Eng. Quart. (Amer. Soc. Met.), August 1965, pp. 1–6.
4. D.C. Ludwigson, Today's Prosthetic Metals, Journal of Metals, Vol. 16, March 1964, pp. 226–231.
5. R.J. Gray, Metallographic Examination of Retrieved Intramedullary Bone Pins and Bone Screws from the Human Body, Report ORNL–TM–4068, Oak Ridge National Laboratory, February 1973.
6. R.J. Gray and L.G. Zirkle Jr., Metallographic -- Examination of a Failed Jewett Nail–Plate from a Human Femur, Microstructural Science, Vol. 4, ed., E.W. Filer, J.M. Hoegfeldt and J. McCall, American Elsevier Publishing Co., Inc., New York, 1976, pp. 179-189.

7. W.E. White and I. Le May, Optical and Electron Fractographic Studies of Fracture in Orthopedic Implants, Microstructure Science, Vol. 3, Part B, American Elsevier Publishing Co., Inc., New York, 1975, pp. 911–930.

8. J.R. Cahoon and H.W. Paxton, Metallurgical Analyses of Failed Orthopedic Implants, J. Biomed Mater Res, Vol. 2, 1968, pp. 1–22.

9. J.H. Dumbleton and E.H. Miller, Failures of Metallic Orthopedic Implants, Metals Handbook, Vol. 10, 8th edition, ASM, 1975, pp. 571–580.

10. Gray, p. 232.

11. B.W. Lisagor, Corrosion and Fatigue of Surgical Implants, ASTM Standardization News, Vol. 3(5), May 1975, pp. 20–24 and 43.

12. Dumbleton and Miller, p. 578.

13. Dumbleton and Miller, p. 577.

14. Dumbleton and Miller, p. 577.

15. A.C. Fraker, A.W. Ruff and M.P. Yeager, Corrosion of Titanium Alloys in Physiological Solutions, Titanium Science and Technology, Year 4, Prenum Pub. Corp., 1973, p. 2447.

16. Lisagor, p. 21.

17. D. Warren, Microstructure and Corrision Resistance of Austenitic Stainless Steels, Presented at Liberty Bell Corrosion Course, NACE and Drexel Institute of Technology, September 1968.

18. Dumbleton and Miller, p. 577.

19. Gray and Zirkle, p. 186.

20. Dumbleton and Miller, p. 577.

21. K.R. Sheeler and L.A. James, Fatigue Behavior of Type 316 Stainless Steel under Simulated Body conditions, J. Biomed Mater Res., Vol. 5, 1971, pp. 267–281.

22. H. W. Russell and W.A. Welcker Jr., Damage and Overstress in the Fatigue of Ferrous Materials, Proc. Am. Soc. Test. Mat., Vol. 36, Part 2, 1936, pp. 118–138.

23. Gray and Zirkle, p. 181.

24. Cahoon and Paxton, p. 16.

25. Lisagor, p. 23.

26. Russell and Welcker Jr., p. 118.

27. B. I. Sander, Foundamentals of Cyclic Stress and Strain, The University of Wisconsin Press, Madison, Wisconsin, 1972, p. 92.

28. Sander, p. 92

29. P.G. Forrest, Fatigue of Metals, Pergamon Press, Oxford, 1962.

30. B. Bresler and J.P. Frankel, Transaction of the ASME, Vol. 72, 1950, pp. 27–36.

31. C.M. Hudson and J.T. Scardina, Engineering Fracture Mechanics, Vol. 1, 1969, p. 429–446.